JOURNAL OF SOLID STATE CHEMISTRY 71, 224–232 (1987)

Chemical Bonding Topology of Superconductors

I. Ternary Molybdenum Chalcogenides (Chevrel Phases)

R. B. KING

Department of Chemistry, University of Georgia, Athens, Georgia 30602

Received August 25, 1986; in revised form February 2, 1987

Models for the chemical bonding topologies of ternary molybdenum chalcogenides (Chevrel phases) are derived using methods based on graph theory. The $M Mo_6S_8$ Chevrel phases as well as their selenium analogs are viewed as three-dimensional lattices of edge-localized discrete Mo_6 octahedra linked electronically through interoctahedral metal–metal interactions. This porously delocalized chemical bonding topology is suggested to be a feature of superconducting systems exhibiting relatively high critical temperatures and magnetic fields. Fusion of molybdenum octahedra through face-sharing leads successively to the Mo_9S_{11} naphthalene analog and the $Mo_{12}S_{14}$ anthracene analog, with increasing fusion leading to increasing delocalization of the chemical bonding topology within individual molybdenum cluster units. The infinite limit of such fusion of molybdenum octahedra corresponds to the infinite chain pseudo-one-dimensional metals $[M_2Mo_6X_6]_\infty$ (M = monovalent metal; X = S, Se, Te) which are formulated with globally delocalized octahedral cavities. Thus the progression from discrete Mo_6 octahedra in the $M Mo_6S_8$ Chevrel phases to the infinite chains of face-fused octahedra in $[M_2Mo_6X_6]_\infty$ leads to a progression from an edge-localized to a globally delocalized chemical bonding topology.

1. Introduction

Several years ago we developed a method based on graph theory (*1*) for the study of the bonding topology in polyhedral boranes, carboranes, and metal clusters (*2, 3*). Subsequent work has shown this method to be very effective in relating electron count to cluster shape for diverse metal clusters using a minimum of computation. Metal clusters treated effectively by this method include post-transition metal clusters (*4*), osmium carbonyl clusters (*5*), gold clusters (*6, 7*), platinum carbonyl clusters (*6, 8*), rhodium carbonyl clusters having fused polyhedra (*9, 10*), and octahedral early transition metal halide clusters (*3, 11*). A recent paper (*11*) shows how this graph theory derived method can be extended to infinite one-dimensional chains and infinite two-dimensional sheets of fused metal octahedra, thereby suggesting the application of this method for the study of solid state materials exhibiting interesting electronic properties, particularly solids containing discrete metal cluster structural units.

This paper describes the first application of our graph theory-derived method to the study of superconducting materials. In this connection Vandenberg and Matthias (*12*) have shown that most high-temperature superconductors contain discrete metal clusters in their crystal lattices, thereby suggesting the relevance of this approach.

The particular superconductors treated in this paper are the ternary molybdenum chalcogenides, commonly known as

0022-4596/87 $3.00

Chevrel phases (*13, 14*). These phases were the first superconducting ternary systems found to have relatively high critical temperatures (*15*), reaching 15 K for $PbMo_6S_8$. In addition the upper critical field of $PbMo_6S_8$ ($H_{c2} \approx 60$ T) is the highest value observed for any class of superconductors (*16, 17*). From the structural point of view the Chevrel phases are constructed from Mo_6 octahedra, which, depending upon the system, can be discrete (i.e., joined only at vertices) and/or fused together (*14*). The discrete Mo_6 octahedra in Chevrel phases may be considered to have a bonding topology analogous to that in the halides $L_6Mo_6X_8^{4+}$ (L = 2-electron donor ligand) which have been treated extensively by both graph theory-derived (*3, 11*) and other (*18–21*) methods. Fusion of molybdenum octahedra in the Chevrel phases involves sharing of opposite triangular faces, similar to some rhodium carbonyl anions (*10*) but different from the sharing of opposite edges found in the infinite chain lanthanide halide clusters such as Gd_2Cl_3 (*11, 22*).

Several theoretical treatments of the Chevrel phases have already been reported, including the tight binding calculations of Mattheiss and Fong (*23*), localized orbital calculations of Bullett (*24*), molecular orbital and band structure calculations by Burdett and Lin (*25*), bond order calculations for the metal–metal bonds by Corbett (*26*), extended Hückel combined molecular orbital and crystal orbital analyses by Hughbanks and Hoffmann (*27*), and several energy-band studies using muffin-tin orbitals (*28, 29*). Strengths of the graph theory-derived method used in this paper include the following:

(1) The ability to deduce important information about the electron counts and shapes of diverse metal clusters using a minimum of computation.

(2) The ability to deduce information concerning the distribution of total cluster electron counts between skeletal bonding within the cluster polyhedron and bonding to external ligands.

(3) The ability to distinguish between localized and delocalized bonding in cluster polyhedra.

The latter two points are potentially important for understanding the electronic properties, including their superconducting properties, of materials built from metal cluster units.

2. Background

The topology of chemical bonding can be represented by a graph in which the vertices correspond to atoms or orbitals participating in the bonding and the edges correspond to bonding relationships. The adjacency matrix **A** of a graph, such as a graph representing chemical bonding, can be defined as follows:

$$A_{ij} = \begin{cases} 0 \text{ if } i = j \\ 1 \text{ if } i \text{ and } j \text{ are connected by an edge} \\ 0 \text{ if } i \text{ and } j \text{ are not connected by an edge} \end{cases} \quad (1)$$

The eigenvalues of the adjacency matrix are obtained from the following determinantal equation:

$$|\mathbf{A} - x\mathbf{I}| = 0, \quad (2)$$

in which **I** is the unit matrix ($I_{ij} = 1$ and $I_{ij} = 0$ for $i \neq j$).

The eigenvalues of the adjacency matrix of the graph representing the relevant chemical bonding correspond to the energy levels of topological molecular orbitals. This approach is related to Hückel theory (*30–33*) which uses the secular equation

$$|\mathbf{H} - \mathbf{ES}| = 0 \quad (3)$$

in which the energy matrix **H** and overlap matrix **S** can be resolved into the unit ma-

trix **I** and the adjacency matrix **A** as follows:

$$\mathbf{H} = \alpha\mathbf{I} + \beta\mathbf{A} \tag{4a}$$

$$\mathbf{S} = \mathbf{I} + \mathbf{SA}. \tag{4b}$$

The Hückel energy levels of the system are related to the eigenvalues x of the adjacency matrix **A** (Eq. (2)) as follows:

$$E = \frac{\alpha + x\beta}{1 + xS}. \tag{5}$$

Thus a positive eigenvalue x of **A** corresponds to a bonding orbital and a negative eigenvalue x corresponds to an antibonding orbital in the corresponding chemical system. In this simple way graph theory can be used to determine the number of bonding and antibonding orbitals for a bonding topology represented by a given adjacency matrix **A**. Such information, although very limited compared with information obtainable at least in principle by more sophisticated methods which are much more complicated computationally, is sufficient to determine favored electron counts for different molecular shapes which are of considerable importance in metal cluster chemistry.

The two extreme types of chemical bonding topology in polyhedral metal clusters may be called *edge localized* and *globally delocalized* (*2*, *3*). An edge-localized polyhedron has two-electron two-center bonds along each edge of the polyhedron. A globally delocalized polyhedron has a multicenter core bond in the center of the polyhedron and may be regarded as a three-dimensional "aromatic" system (*34*). A complicated metal cluster system consisting of fused and/or capped polyhedra can have globally delocalized bonding in some polyhedral regions and edge-localized bonding in other polyhedral regions.

One of the major achievements of the graph theory-derived approach to the chemical bonding topology in globally delocalized systems is the demonstration of the close analogy between the bonding in two-dimensional planar polygonal aromatic systems such as benzene and that in three-dimensional deltahedral boranes and carboranes (*2*), where a *deltahedron* is a polyhedron in which all faces are triangles. The latter three-dimensional structures are topologically equivalent to metal cluster structures through ideas first presented by Wade in 1971 (*35*) and subsequently developed extensively by Hoffmann as isolobality (*36*).

Consider a globally delocalized polygonal or deltahedral system having n vertices. The skeletal bonding topology of such a system involves three valence orbitals from each vertex atom which are known (*2*) as *internal orbitals*. The set of three internal orbitals on each vertex atom is divided into two twin or tangential internal orbitals and one unique or radial internal orbital. Pairwise overlap between the $2n$ twin internal orbitals is responsible for the formation of the polygonal or deltahedral framework and leads to the splitting of the $2n$ orbitals into n bonding and n antibonding orbitals, thereby providing surface bonding in the case of globally delocalized deltahedra. This bonding is supplemented by additional bonding and antibonding orbitals formed by global mutual overlap of the n unique internal orbitals. This overlap can be represented by a graph G in which the vertices correspond to the vertex atoms or, equivalently, their unique internal orbitals and the edges represent pairs of overlapping unique internal orbitals. The relative energies of the additional molecular orbitals arising from such overlap of the unique internal orbitals are determined from the eigenvalues x of the adjacency matrix **A** of the graph G (see Eqs. (2) and (5) above). In the case of benzene the graph G is the C_6 graph (hexagon) which has three positive and three negative eigenvalues corresponding to the three π bonding and three π^* antibonding

orbitals, respectively. In the case of a globally delocalized deltahedron having n vertices such as found in deltahedral boranes $B_nH_n^{2-}$ and carboranes $C_2B_{n-2}H_n$ ($6 \leq n \leq 12$) as well as some octahedral metal clusters ($n = 6$), the graph G is the complete graph K_n in which each of the vertices has an edge going to every other vertex for a total of $n(n-1)/2$ edges. This corresponds to an n-center bond at the center (core) of the deltahedron formed by overlap of each unique internal orbital with every other unique internal orbital. The complete graph K_n has one positive eigenvalue and $n-1$ negative eigenvalues regardless of the value of n, indicating that the n-center core bond in a globally delocalized deltahedral cluster leads to only one new bonding molecular orbital. Thus the overlap of the *unique* internal orbitals in both the two-dimensional polygonal and the three-dimensional deltahedral globally delocalized systems leads to an *odd* number of additional bonding molecular orbitals corresponding to $4k + 2$ π-electrons for the polygonal systems. The core bonding of the globally delocalized deltahedral systems also follows the $4k + 2$ electron rule with $k = 0$. Furthermore, the sum of the n bonding orbitals arising from the surface bonding of the twin internal orbitals and the single bonding orbital arising from the n-center core bonding of the unique internal orbitals gives a total of $n + 1$ bonding orbitals for globally delocalized deltahedra having n vertices. Filling these $n + 1$ bonding orbitals with electron pairs in the usual way gives a total of $2n + 2$ skeletal bonding electrons in accord with the observed number in stable globally delocalized deltahedral boranes, carboranes, and metal clusters. Further details of this bonding model are presented elsewhere (*2, 3*). In addition, recent work (*37*) indicates that for globally delocalized octahedral boranes this simple graph theory-derived model gives results consistent with simple extended Hückel calculations.

The relationship between the number of edges meeting at a vertex (the vertex degree) and the number of internal orbitals used by the atom at the vertex in question determines whether or not the bonding in the polyhedral cluster is edge localized or globally delocalized (*3*). Thus edge-localized bonding requires that all vertex degrees match the number of internal orbitals used by the corresponding vertex atoms. Conversely, delocalization occurs when there is a mismatch between the vertex degrees of the polyhedron and the numbers of internal orbitals provided by the corresponding vertex atoms. Since the above model for globally delocalized cluster bonding requires three internal orbitals from each vertex, the smallest globally delocalized polyhedron is the regular octahedron, which is the smallest polyhedron having no vertices of degree 3. Metal octahedra, whether globally delocalized using three internal orbitals from each vertex atom or edge localized using four internal orbitals from each vertex atom, are frequently encountered building blocks for metal clusters, including the Chevrel phases discussed in this paper. Relationships between edge-localized and globally delocalized metal octahedra as well as face-localized metal octahedra involving an intermediate degree of delocalization have been discussed for early transition metal halides (*11*) and will be reviewed in the next section in preparation for the discussion of the chemical bonding topology of Chevrel phases.

The extended Hückel treatment of Hughbanks and Hoffmann (*27*) considers the closed-shell electronic configurations of the metal cluster building blocks of the Chevrel phase structures. The treatment of this paper likewise starts from these closed-shell electronic configurations and develops a model for their chemical bonding topologies. The actual Chevrel phases have effective electron counts per cluster unit one to

two electrons less than the closed-shell electronic configurations of the individual cluster units, thereby providing the partially filled energy bands required for their conducting properties. In addition, intercluster metal–metal interactions in the Chevrel phases provide electronic bridges between the individual discrete metal cluster units which also are essential for the conducting properties.

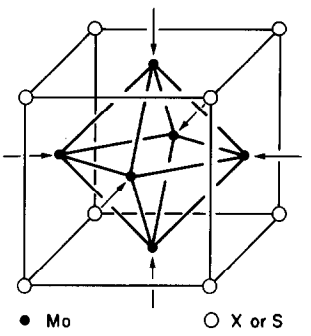

FIG. 1. The Mo_6 octahedron within a halogen or chalcogen cube as a building block for the octahedral molybdenum clusters discussed in this paper. Arrows indicate sites of coordination with external ligands, halogens, or chalcogens from adjacent metal cluster units.

3. Discrete Octahedra

The octahedral metal cluster building blocks for the Chevrel phases are closely related to certain early transition metal halides built from discrete octahedral metal clusters which have been discussed in recent papers (*11, 21*). The two complementary types (*11, 21*) of such clusters are the face-bridged, edge-localized $Mo_6X_8L_6^{4+}$ and the edge-bridged, face-localized $Nb_6X_{12}L_6^{2+}$; the discrete octahedral molybdenum clusters of the Chevrel phases are analogous to the former and also have electronic configurations consistent with an edge-localized bonding topology.

The prototypical examples of edge-localized octahedral metal cluster halides are the molybdenum(II) halide derivatives generally represented as $Mo_6X_8L_6^{4+}$, including "molybdenum dichloride," $Mo_6(\mu_3\text{-}Cl)_8Cl_2Cl_{4/2}$ (*38*). The structures of these compounds consist of Mo_6 octahedra, a face-bridging (μ_3) halogen atom in each of the eight faces of the Mo_6 octahedra, and one bond from each molybdenum vertex to an external ligand (L), which may be a halogen atom bridging to another Mo_6 octahedron. The eight halogen atoms capping the faces of a given Mo_6 octahedron thus form a cube surrounding the Mo_6 octahedron (Fig. 1). Each *neutral* halogen vertex functions as a donor of five skeletal electrons, leaving an electron pair to function as a ligand to a molybdenum atom in an adjacent octahedron. The vertex molybdenum atoms are nine-coordinate using a four-capped square antiprism coordination polyhedron (*11*) with the external ligand in the axial position, four bonds to face-bridging halogen atoms in the four medial positions, and the four internal orbitals in the basal positions forming the two-center bonds with the adjacent molybdenum atoms in the Mo_6 octahedron. An LMo vertex using four internal orbitals and thus five external orbitals is a (5)(2) − 6 − 2 = 2 electron acceptor (or −2 electron donor) after allowing 6 electrons from the neutral molybdenum atom and 2 electrons from the neutral external ligand L. This leads to the following electron-counting scheme (*3, 11*):

6 LMo vertices (6)(−2) =	−12 electrons
8 μ_3-X bridges (8)(5) =	40 electrons
+4 charge	−4 electrons
Total skeletal electrons	24 electrons

These 24 skeletal electrons are exactly the number required for an edge-localized octahedron having two-center bonds along each of its 12 edges.

Now consider the Chevrel phases of the general formulas $M_nMo_6S_8$ and $M_nMo_6Se_8$ (M = Ba, Sn, Pb, Ag, lanthanides, Fe, Co, Ni, etc.). The basic building blocks of their

structures are Mo_6S_8 (or Mo_6Se_8) units containing a bonded Mo_6 octahedron (Mo–Mo distances in the range 2.67 to 2.78 Å) with a sulfur atom capping each face, leading to an Mo_6 octahedron within an S_8 cube as depicted in Fig. 1. Each (neutral) sulfur atom of the S_8 cube functions as a donor of four skeletal electrons to the Mo_6 octahedron within that S_8 cube, leaving an electron pair to function as a ligand to a molybdenum atom in an adjacent Mo_6 octahedron. Maximizing this sulfur electron pair donation to the appropriate molybdenum atom in the adjacent Mo_6 octahedron results in a tilting of the Mo_6 octahedron by about 25° within the cubic array of the other metal atoms *M*. These other metal atoms *M* furnish electrons to the Mo_6S_8 units allowing them to approach but not attain the $Mo_6S_8^{4-}$ closed-shell electronic configuration. This corresponds to a partially filled conduction band. Electronic bridges between individual Mo_6 octahedra are provided by interoctahedral metal–metal interactions (nearest *inter*octahedral Mo–Mo distances in the range 3.08 to 3.49 Å for Mo_6S_8 and Mo_6Se_8 derivatives (*13*)).

The $Mo_6S_8^{4-}$ closed-shell electronic configuration for the fundamental Chevrel phase building block is isoelectronic with that of the $Mo_6X_8L_6^{4+}$ halides discussed above, remembering that each molybdenum vertex receives an electron pair from a sulfur atom of an adjacent Mo_6S_8 unit and thus may be treated as an *L*Mo vertex. This leads to the following electron counting scheme for the closed-shell $Mo_6S_8^{4-}$ unit:

6 *L*Mo vertices (6)(−2) =	−12 electrons
8 μ_3-*S* bridges (8)(4) =	32 electrons
−4 charge	4 electrons
Total skeletal electrons	24 electrons

These 24 skeletal electrons are again the exact number required for an edge-localized octahedron having two-center bonds along each of the 12 edges.

4. Fusion of Octahedra

The Chevrel phases include not only species constructed from discrete Mo_6S_8 (or Mo_6Se_8) octahedra but also species constructed from Mo_9S_{11}, $Mo_{12}S_{14}$, and $(Mo_6S_6)_\infty$ units formed by the fusion of octahedra by sharing triangular faces. This fusion process may be regarded as analogous to the formation of polycyclic aromatic hydrocarbons from the fusion of hexagons by sharing edges. This suggests the classification of fused molybdenum octahedra by the trivial name of the polycyclic benzenoid hydrocarbon having an analogous configuration of its planar hexagon building blocks as depicted in Fig. 2. A similar scheme has recently been suggested for the treatment of rhodium carbonyl clusters having related structures based on face-fused octahedra (*10*).

The molybdenum atoms in the fused octahedra of Fig. 2 are of two types, inner and outer. Outer molybdenum atoms are similar to those in the discrete octahedral Mo_6S_8

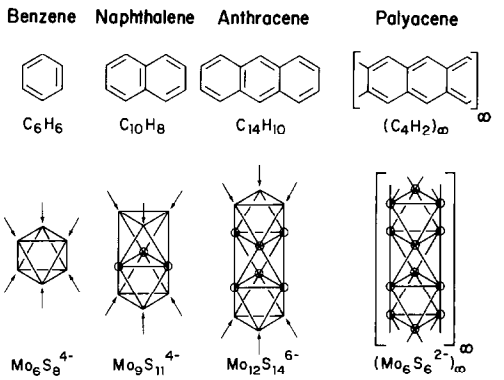

FIG. 2. Analogy between the fusion of molybdenum octahedra in ternary molybdenum sulfide structures and the fusion of benzene rings in planar polycyclic aromatic hydrocarbons. Uncircled vertices are outer molybdenum atoms and circled vertices are inner molybdenum atoms. Arrows indicate sites of coordination with sulfur atoms of adjacent metal cluster units. Sulfur atoms are omitted for clarity. Similar structural units are present in analogous molybdenum selenides and tellurides.

building blocks discussed above. They thus use four internal orbitals and receive an electron pair from a sulfur atom of an adjacent metal cluster unit (indicated by arrows in Fig. 2). The inner molybdenum atoms (circled in Fig. 2) use six internal orbitals and do *not* receive an electron pair from a sulfur atom of an adjacent metal cluster. They are therefore zero electron donors ((3)(2) − 6 − 0). Edges connecting pairs of inner molybdenum atoms are bridged by sulfur atoms but these sulfur atoms also bond to one molybdenum atom in each adjacent Mo_3 triangle (above and below in Fig. 2) so that they function as pseudo-5-coordinate μ_4 sulfur atoms and donors of four skeletal electrons to their own cluster units. Thus all sulfur atoms in the species depicted in Fig. 2 function as four-electron donors when considered as neutral ligands to a single aggregation of face-fused Mo_6 octahedra. The electron and orbital counting of these systems can then proceed as follows considering only orbitals involved in the metal–metal bonding:

1. Naphthalene Analog, $Mo_9S_{11}^{4-}$

Source of skeletal orbitals and electrons:

6 outer *L*Mo vertices	24 orbitals	−12 electrons
3 inner Mo vertices	18 orbitals	0 electrons
11 S atoms		44 electrons
−4 charge		4 electrons
Totals available for skeletal bonding	42 orbitals	36 electrons

Use of skeletal orbitals and electrons for metal–metal bonding of various types:

6 edge bonds on outer triangles	12 orbitals	12 electrons
6 face bonds connecting inner and outer triangles	18 orbitals	12 electrons
6 edge bonds connecting inner and outer triangles	12 orbitals	12 electrons
Totals used in skeletal bonding	42 orbitals	36 electrons

Note that the bonding topology of $Mo_9S_{11}^{4-}$ contains three three-center Mo–Mo–Mo face bonds in each of the two octahedra between an outer and inner Mo_3 triangle similar to the three-center Nb–Nb–Nb face bonds in the $Nb_6X_{12}L_6^{2+}$ mentioned above and discussed in more detail elsewhere (*11*, *21*).

2. Anthracene Analog, $Mo_{12}S_{14}^{6-}$

Source of skeletal orbitals and electrons:

6 outer *L*Mo vertices	24 orbitals	−12 electrons
6 inner Mo vertices	36 orbitals	0 electrons
14 S atoms		56 electrons
−6 charge		6 electrons
Totals available for skeletal bonding	60 orbitals	50 electrons

Use of skeletal orbitals and electrons for metal–metal bonding of various types:

Globally delocalized Mo_6 octahedron		
Surface bonding	12 orbitals	12 electrons
Core bonding	6 orbitals	2 electrons
Outer Mo_3 triangles		
6 edge bonds	12 orbitals	12 electrons
Octahedra formed by an outer and an inner Mo_3 triangle		
6 face bonds	18 orbitals	12 electrons
6 edge bonds	12 orbitals	12 electrons
Totals used in skeletal bonding	60 orbitals	50 electrons

This bonding model suggests that of the three octahedral cavities in the $Mo_{12}S_{14}^{6-}$ structure, the octahedral cavity formed by the two inner Mo_3 triangles has globally delocalized bonding whereas the two equivalent octahedral cavities formed by one outer and one inner Mo_3 triangle have the same combination of two-center (edge) and three-center (face) bonds as the two (equivalent) octahedral cavities in the $Mo_9S_{11}^{4-}$ cluster discussed above.

Continuation of this principle of face-fused octahedra predicts the existence of a homologous series with the general formula $Mo_{3+3n}S_{5+3n}^{2n-}$ in which the *difference* between the numbers of atomic orbitals and electrons available for skeletal bonding follows a $4(n - 1) + 2$ rule, where n is the

number of octahedral cavities. The known face-fused octahedral molybdenum chalcogenide clusters depicted in Fig. 2 consist of linearly fused metal octahedra analogous to the series benzene, naphthalene, anthracene, naphthacene, etc. Angularly fused metal octahedra analogous to phenanthrene are possible in principle but so far have not been observed.

The limit of the face-sharing fusion of molybdenum octahedra is the linear polyacene analogs $(Mo_6S_6^{2-})_\infty$ (Fig. 2) known in a number of derivatives $[M_2Mo_6S_6]_\infty$ (M = K, Rb, Cs) as well as the selenium analogs $[M_2Mo_6Se_6]_\infty$ (M = Na, K, Rb, Cs, Tl, Ag) and the tellurium analog $[M_2Mo_6Te_6]_\infty$ (M = Rb, Cs, In, Tl) (*39, 40*). The structures of these systems consist of infinite chains of face-fused octahedra. All molybdenum atoms are inner molybdenum atoms and none of the chalcogens bridge to other chains so that there are no close contacts between the different chains. In accord with this structure these systems function as pseudo-one-dimensional metals with strongly anisotropic conductivities several hundred times larger parallel to the chains of octahedra relative to the perpendicular directions (*39, 41*). The $Mo_{6/2}S_{6/2}^{-}$ octahedra serving as building blocks for these $[M_2Mo_6S_6]_\infty$ derivatives and their selenium and tellurium analogs have 13 skeletal electrons, i.e., none from the (inner) molybdenum vertices, 12 (= (3)(4)) from the three sulfur atoms, and 1 from the -1 charge. These 13 skeletal electrons per $Mo_{6/2}S_{6/2}^{-}$ are one less than the 14 skeletal electrons required for the octahedral cavity to be globally delocalized ($2v + 2 = 14$ for $v = 6$). These holes in the closed-shell electronic configurations for globally delocalized $[Mo_6S_6^{2-}]_\infty$ provide a mechanism for electronic conduction along the chains of face-fused octahedra. Peierls distortions (*42, 43*) leading to alternately long and short spaces between the Mo_3X_3 (X = S, Se, Te) units in the chains of fused octahedra appear to be relatively unfavorable for these systems but have been suggested (*40, 44*) to account for the broad metal–semiconductor transitions in the ternary molybdenum tellurides $[M_2Mo_6Te_6]_\infty$ (M = Rb, Cs).

5. Conclusion

The chemical bonding topology of the Chevrel phases MMo_6S_8 consisting of edge-localized discrete Mo_6 octahedra linked through sulfur atoms as well as interoctahedral metal–metal interactions leads naturally to the concept of *porous delocalization*. Thus the bonding in a polyhedron with edge-localized bonding is porous in contrast to the dense bonding in a polyhedron with globally delocalized bonding. In other words porous chemical bonding involves only the 1-skeleton (*45*) of the polyhedron in contrast to dense chemical bonding which involves the whole volume of the polyhedron. An interesting refinement of the ideas of Vandenberg and Matthias (*12*) arising from this analysis of the chemical bonding topology of the Chevrel phases as well as that of the ternary rhodium borides in the subsequent paper is the conjecture that a porously delocalized three-dimensional network consisting of electronically linked polyhedral metal clusters having edge-localized chemical bonding leads to superconducting systems having relatively high critical fields and temperatures. Thus the porosity of the chemical bonding in these systems makes their superconductivity less susceptible to magnetic fields and temperature than that of densely delocalized systems such as pure metals. This idea appears to be related to the suggestion (*46*) that the high critical field of the Chevrel phases is due to a certain localization of the conduction-electron wavefunction of the Mo_6 clusters, leading to an extremely short mean free path and/or a low Fermi velocity corresponding to a small BCS coherence length.

The other interesting conclusion from this paper is that fusion of octahedra by face-sharing increases the delocalization of their chemical bonding topology. Thus the discrete Mo_6 octahedra in the MMo_6S_8 Chevrel phases exhibit edge-localized bonding whereas the $Mo_{6/2}$ octahedral units in the $[M_2Mo_6S_6]_\infty$ infinite chains of face-sharing octahedra exhibit globally delocalized bonding.

Acknowledgment

We are indebted to the Office of Naval Research for partial support of this work.

References

1. N. TRINAJSTIĆ, "Chemical Graph Theory" CRC Press, Boca Raton, FL (1983).
2. R. B. KING AND D. H. ROUVRAY, *J. Amer. Chem. Soc.* **99,** 7834 (1977).
3. R. B. KING, *in* "Chemical Applications of Topology and Graph Theory" (R. B. King, Ed.), pp. 99–123. Elsevier, Amsterdam (1983).
4. R. B. KING, *Inorg. Chim. Acta* **57,** 79 (1982).
5. R. B. KING, *Inorg. Chim. Acta* **116,** 99 (1986).
6. R. B. KING, *in* "Mathematics and Computational Concepts in Chemistry" (N. Trinajstić, Ed.), pp. 146–154. Ellis Horwood, Chichester (1986).
7. R. B. KING, *Inorg. Chim. Acta* **116,** 108 (1986).
8. R. B. KING, *Inorg. Chim. Acta* **116,** 119 (1986).
9. R. B. KING, *Inorg. Chim. Acta* **116,** 125 (1986).
10. R. B. KING, *Int. J. Quant. Chem.* **205,** 227 (1986).
11. R. B. KING, *Inorg. Chim. Acta* **129,** 91 (1987).
12. J. M. VANDENBERG AND B. T. MATTHIAS, *Science* **198,** 195 (1977).
13. Ø. FISCHER, *Appl. Phys.* **16,** 1 (1978).
14. R. CHEVREL, P. GOUGEON, M. POTEL, AND M. SERGENT, *J. Solid State Chem.* **57,** 25 (1985).
15. B. T. MATTHIAS, M. MAREZIO, E. CORENZWIT, A. S. COOPER, AND H. E. BARZ, *Science* **175,** 1465 (1972).
16. Ø. FISCHER, H. JONES, G. BONGI, M. SERGENT, AND R. CHEVREL, *J. Phys. C* **7,** L450 (1974).
17. S. FONER, E. J. MCNIFF, JR., AND E. J. ALEXANDER, *Phys. Lett. A* **49,** 269 (1974).
18. F. A. COTTON AND T. E. HAAS, *Inorg. Chem.* **3,** 10 (1964).
19. L. J. GUGGENBERGER AND A. W. SLEIGHT, *Inorg. Chem.* **8,** 2041 (1969).
20. R. G. WOOLLEY, *Inorg. Chem.* **24,** 3519 (1985).
21. R. L. JOHNSTON AND D. M. P. MINGOS, *Inorg. Chem.* **25,** 1661 (1986).
22. D. A. LOKKEN AND J. D. CORBETT, *Inorg. Chem.* **12,** 556 (1973).
23. L. F. MATTHEISS AND C. Y. FONG, *Phys. Rev. B* **15,** 1760 (1977).
24. D. W. BULLETT, *Phys. Rev. Lett.* **39,** 664 (1977).
25. J. A. BURDETT AND J.-H. LIN, *Inorg. Chem.* **21,** 5 (1982).
26. J. D. CORBETT, *J. Solid State Chem.* **39,** 56 (1981).
27. T. HUGHBANKS AND R. HOFFMANN, *J. Amer. Chem. Soc.* **105,** 1150 (1983).
28. O. K. ANDERSEN, W. KLOSE, AND H. NOHL, *Phys. Rev. B* **17,** 1209 (1978).
29. T. JARLBORG AND A. J. FREEMAN, *Phys. Rev. Lett.* **44,** 178 (1980).
30. K. RUEDENBERG, *J. Chem. Phys.* **22,** 1878 (1954).
31. H. H. SCHMIDTKE, *Coord. Chem. Rev.* **2,** 3 (1967).
32. H. H. SCHMIDTKE, *J. Chem. Phys.* **45,** 3920 (1966).
33. I. GUTMAN AND N. TRINAJSTIĆ, *Top. Curr. Chem.* **42,** 49 (1973).
34. J. AIHARA, *J. Amer. Chem. Soc.* **100,** 3339 (1978).
35. K. WADE, *Chem. Commun.*, 792 (1971).
36. R. HOFFMANN, *Angew. Chem. Int. Ed.* **21,** 711 (1982).
37. R. B. King, *J. Comput. Chem.* **8,** 341 (1987).
38. H. SCHÄFER, H. SCHNERING, J. TILLACK, F. KUHNEN, H. WÖHLRE, AND H. BAUMANN, *Z. Anorg. Allg. Chem.* **353,** 281 (1965).
39. M. POTEL, R. CHEVREL, M. SERGENT, J. C. ARMICI, M. DECROUX, AND Ø. FISCHER, *J. Solid State Chem.* **35,** 286 (1980).
40. P. H. HOR, W. C. FAN, L. S. CHOU, R. L. MENG, C. W. CHU, J. M. TARASCON, AND M. K. WU, *Solid State Commun.* **55,** 231 (1985).
41. J. C. ARMICI, M. DECROUX, Ø. FISCHER, M. POTEL, R. CHEVREL, AND M. SERGENT, *Solid State Commun.* **33,** 607 (1980).
42. J. S. MILLER AND A. J. EPSTEIN, *Prog. Inorg. Chem.* **20,** 1 (1976).
43. T. HUGHBANKS AND R. HOFFMANN, *Inorg. Chem.* **21,** 3578 (1982).
44. J. M. TARASCON, F. J. DISALVO, AND J. V. WASZACZAK, *Solid State Commun.* **52,** 227 (1984).
45. B. GRÜNBAUM, "Convex Polytopes." Interscience, New York (1967).
46. Ø. FISCHER, M. DECROUX, R. CHEVREL, AND M. SERGENT, *in* "Superconductivity in *d*- and *f*-Band Metals" (D. H. Douglas, Ed.), pp. 176–177. Plenum Press, New York (1976).